Peristaltic flow of micropolar fluid with nanoparticles through porous medium under the effects of heat absorption, chemical reaction and wall properties

Shaimaa F. Ramadan

Department of mathematics, Faculty of Science (Girls), Al-Azhar University, Nasr-City, Cairo, Egypt

Abstract

In the present analysis we have discussed the effects of heat absorption, chemical reaction and wall properties on peristaltic flow of micropolar nanofluid through a porous medium. The fundamental equations of the motion are first modulated and then simplified under the assumptions of long wavelength and low Reynolds number. The exact solutions have been calculated for the velocity and the microrotation velocity, while the governing equations of energy and nanoparticles equations are solved analytically using homotopy perturbation method. In the end, graphical results are discussed to illustrate the effects of various physical parameters of the problem on these distributions.

1. Introduction

Nanoparticle-fluid suspensions are termed nanofluids, obtained by dispersing nanometer sized particles in a conventional base fluid water, oil and ethylene glycol. Nanoparticles of materials such as metallic oxides, nitride ceramics, carbide ceramics and metals have been used for the preparation of nanofluids. These nanofluids have been found to possess an enhanced thermal conductivity as well as improved heat transfer performance. Also, cooling is indispensable for maintaining the desired performance and reliability of a wide variety of industrial products such as computers, power electronic circuits, X-ray generators and wind turbines [1]. With the unprecedented increase in heat loads and heat fluxes caused by more power in miniaturized products, high tech industries such as microelectronics, transportation and defense face cooling as one of the top technical challenges. For example, the electronics industry has provided computers with faster speed, smaller size and expanded futures, leading to reduce heat loads, heat fluxes and localized hot spots at the chip and package levels. Peristaltic transport of a nanofluid in an inclined tube has been addressed by Prasad et. al. [2]. Nowar [3] studied

the peristaltic flow of nanofluid under the effect of hall current and porous medium. Consequences of nanofluid on peristaltic flow in an asymmetric channel is analyzed by Nadeem et. al. [4]. Mahbubul et. al. [5] investigated latest developments on the viscosity of nanofluids. Mustafa et. al. [6] obtained analytical and numerical solutions of the influence of wall properties on the peristaltic flow of a nanofluid. Numerical solution of peristaltic flow of a Carreau nanofluid in asymmetric channel obtained by Akbar et. al. [7]. Krishnamurthy et. al. [8] discussed the effect of chemical reaction on MHD boundary layer flow and melting heat transfer of Williamson nanofluid in porous medium.

The theory of micropolar fluids introduced by Eringen [9] deals with a class of fluids which exhibit the micro-rotational effects and micro-rotational inertia. Physically, micropolar fluids may represent fluids consisting of rigid, randomly oriented (spherical) particles suspended in a viscous medium, where the deformation of fluid particles is ignored. The micropolar fluid theory has been successfully applied to the analysis of the wide variety of flow problems in fluid mechanics. The theory of micropolar fluid includes the effects of local rotary inertia and couple stress is expected to provide a mathematical model for the non-Newtonian behavior observed certain man-made liquids such theologically complex fluid as liquid crystals. Nadeem et. al. [10] analyzed the axisymmetric stagnation flow of micropolar nanofluid in a moving cylinder. Numerical study of micropolar convective heat and mass transfer in a non-Darcy porous regime with Soret and Dufour diffusion effects is introduced by Beg et. el. [11]. Flow of a micropolar fluid on a continuous moving surface is made by Ishak et. al. [12]. Bakier [13] investigated the natural convection heat and mass transfer in a micropolar fluid-saturated non-Darcy porous regime with radiation and thermophoresis effects. Stokes flow of micropolar fluids by peristaltic pumping though tube with slip boundary condition is studied by Tripathi et. al. [14]. Biswas et. al. [15] examined MHD micropolar fluid flow through vertical plate with heat generation. Peristaltic transport of micropolar fluid in a tubes under influence of magnetic field and rotation is introduced by Abd-Alla et. al. [16]. Effect of suction/injection on flow of micropolar fluid past a continuously moving plate in the presence of radiation is discussed by El-Arabawy [17]. Abou-zeid [18] analyzed the effects of thermal-diffusion and viscous dissipation on peristaltic flow of micropolar non-Newtonian nanofluid: application of homotopy perturbation method. The

wall properties effect on peristaltic transport of micropolar non-Newtonian fluid with heat and mass transfer is studied by Eldabe and Abou-zeid [19].

Peristaltic transport is a form of material transport induced by a progressive wave of area contraction or expansion along the length of a distensible tube, mixing and transporting the fluid in the direction of the wave propagation. This mechanism has received considerable attention in recent times in engineering as well as in medicine. It plays indispensable role in transporting many physiological fluids in body. Many modern mechanical devices have been designed on the principle of peristaltic pumping for transporting noxious fluids without contaminating the internal parts. Sankad and Radhakrishnamacharya [20] investigate the influence of wall properties on the peristaltic motion of a Herschel-Bulkley fluid in channel. Flow of Herschel-Bulkley fluid in an inclined flexible channel lined with porous material under peristalsis is studied by Sreenadh et. al. [21]. The effect of heat transfer on peristaltic transport of a Newtonian fluid through a porous medium in an asymmetric vertical channel is studied by Vasudev [22]. Peristaltic flow of a Newtonian fluid through a porous medium in a vertical tube under the effect of magnetic field is studied by Vasudev et. al. [23]. The flow separation through peristaltic motion for Power-law fluid in uniform tube is studied and reported by Abd El Naby and Abd El Kareem [24]. Hayat and Javed [25] obtained the exact solutions of peristaltic transport of Power-law fluid in asymmetric channel with compliant walls. Peristaltic flow of Williamson fluid in an asymmetric channel through porous medium is analyzed by Kavitha et. al. [26]. Hayat et. al. [27] discussed the heat transfer analysis for peristaltic mechanism in variable viscosity fluid.

The aim of the current study is to discuss the peristaltic transport of micropolar nanofluid through porous medium in a symmetric horizontal channel under the effects of heat absorption, chemical reaction and wall properties. The fundamental equations which govern this flow have been modulated under long wavelength and low Reynolds number assumptions, a closed form solution for velocity and microrotation velocity are presented. Homotopy perturbation solutions for energy and nanoparticles equations are obtained. The physical behaviors of emerging parameters are discussed through the graphs.

2. Mathematical formulation

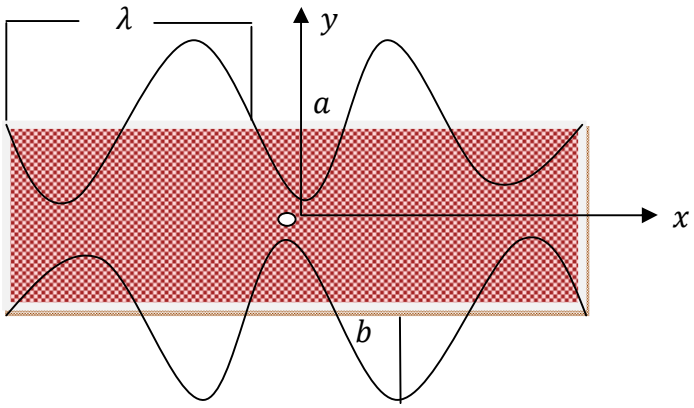

Figure (1) The sketch of the problem

We consider the peristaltic transport of micropolar fluid with nanoparticles through porous medium in a symmetric two-dimensional channel with flexible walls on which are imposed traveling sinusoidal waves of long wavelength. The lower and upper walls of the channel are maintained at constant temperature (T_o and T_1) and nanoparticles volume fraction (φ_o and φ_1). Figure (1) shows the physical model of a symmetric channel.

The channel wall equation is given by:

$$h = a + b \sin\left(\frac{2\pi}{\lambda}(x - ct)\right) \tag{1}$$

Where a is the half width of the channel, b is the amplitude of the wave, λ is the wavelength, t is the time and c is the wave velocity.

The equation of motion of the flexible wall is given by:

$$L(\eta) = P - P_O \tag{2}$$

Where L is an operator that is used to represnt the motion of the stretched membrance with damping forces such that:

$$L = -T_2 \frac{\partial^2}{\partial x^2} + M_2 \frac{\partial^2}{\partial t^2} + C_2 \frac{\partial}{\partial t} \tag{3}$$

Where T_2 is the tension in the membrane, M_2 is the mass per unit area, C_2 is the coefficient of the damping force and P_O is the pressure on the outside of the wall due to tension in the muscles.

If we assume that $P_O = 0$, then the equations governing the two-dimensional transport of incompressible micropolar fluid with nanoparticles through a porous medium in a symmetric channel are:

$$\frac{\partial u}{\partial x} + \frac{\partial v}{\partial y} = 0 \tag{4}$$

$$\rho_f \left[u\frac{\partial u}{\partial x} + v\frac{\partial u}{\partial y}\right] = -\frac{\partial P}{\partial x} + k\frac{\partial \Omega}{\partial y} + (k+\mu)\left[\frac{\partial^2 u}{\partial x^2} + \frac{\partial^2 u}{\partial y^2}\right] - \frac{\mu}{k_1}u \tag{5}$$

$$\rho_f \left[u\frac{\partial v}{\partial x} + v\frac{\partial v}{\partial y}\right] = -\frac{\partial P}{\partial y} + k\frac{\partial \Omega}{\partial x} + (k+\mu)\left[\frac{\partial^2 v}{\partial x^2} + \frac{\partial^2 v}{\partial y^2}\right] - \frac{\mu}{k_1}v \tag{6}$$

$$\rho_f J\left[u\frac{\partial \Omega}{\partial x} + v\frac{\partial \Omega}{\partial y}\right] - 2k\Omega + k\left[\frac{\partial v}{\partial x} - \frac{\partial u}{\partial y}\right] + \gamma_1\left[\frac{\partial^2 \Omega}{\partial x^2} + \frac{\partial^2 \Omega}{\partial y^2}\right] \tag{7}$$

$$(\rho c)_f\left[u\frac{\partial T}{\partial x} + v\frac{\partial T}{\partial y}\right] = k_T\left[\frac{\partial^2 T}{\partial x^2} + \frac{\partial^2 T}{\partial y^2}\right] + (\rho c)_p\left[D_B\left(\frac{\partial \varphi}{\partial x}\frac{\partial T}{\partial x} + \frac{\partial \varphi}{\partial y}\frac{\partial T}{\partial y}\right) + \frac{D_T}{T_o}\left(\left(\frac{\partial T}{\partial x}\right)^2 + \left(\frac{\partial T}{\partial y}\right)^2\right)\right] - Q_o(T - T_O) \tag{8}$$

$$\left[u\frac{\partial \varphi}{\partial x} + v\frac{\partial \varphi}{\partial y}\right] = D_B\left[\frac{\partial^2 \varphi}{\partial x^2} + \frac{\partial^2 \varphi}{\partial y^2}\right] + \frac{D_T}{T_o}\left[\frac{\partial^2 T}{\partial x^2} + \frac{\partial^2 T}{\partial y^2}\right] - k_2(\varphi - \varphi_o) \tag{9}$$

Where u and v are velocity component, ρ_f is the density of the fluid, P is the pressure, k is the micropolar viscosity, Ω is the microrotation velocity, μ is the viscosity, k_1 is the permeability of porous medium, J is the microinertia constant, γ_1 is material constant, $(\rho c)_f$ is the heat capacity of the fluid, $(\rho c)_p$ is the heat capacity of the nanoparticle material, k_T is the thermal conductivity, D_B is the Brownian diffusion coefficient, D_T is the thermophoretic coeffecient, Q_o is the heat absorption coefficient and k_2 is the chemical reaction parameter.

The appropriate boundary conditions are:

$$u = 0,\ \Omega = 0,\quad T = T_o \text{ and } \varphi = \varphi_o \text{ at } y = -h \Big\}$$

$$u = 0\,,\ \Omega = 0\,,\ T = T_1 \text{ and } \varphi = \varphi_1 \quad \text{at} \quad y = h \tag{10}$$

Let us introduce the following dimensionless quantities as:

$$x^* = \frac{x}{\lambda}\,,\ y^* = \frac{y}{a}\,,\ h^* = \frac{h}{a}\,, t^* = \frac{tc}{\lambda}\,,\ u^* = \frac{u}{c}\ , v^* = \frac{v}{c\delta}\,,\ \delta = \frac{a}{\lambda}\,, P^* = \frac{Pa^2}{\mu\lambda c}\,, \Omega^* = \frac{\Omega a}{c}\,,$$
$$J^* = \frac{J}{a^2}\,, \theta = \frac{T-T_o}{T_1-T_o}\ ,\ \varphi^* = \frac{\varphi-\varphi_o}{\varphi_1-\varphi_o}\,. \tag{11}$$

After substituting from (10), Equations (5-9) can be written in dimensionless form after dropping the star mark as:

$$Re\ \delta\left[u\frac{\partial u}{\partial x} + v\frac{\partial u}{\partial y}\right] = -\frac{\partial P}{\partial x} + \frac{k}{\mu}\frac{\partial \Omega}{\partial y} + \frac{k+\mu}{\mu}\left[\delta^2\frac{\partial^2 u}{\partial x^2} + \frac{\partial^2 u}{\partial y^2}\right] - \frac{a^2}{k_1}u \tag{12}$$

$$Re\ \delta^3\left[u\frac{\partial v}{\partial x} + v\frac{\partial v}{\partial y}\right] = -\frac{\partial P}{\partial y} + \delta^2\frac{k}{\mu}\frac{\partial \Omega}{\partial x} + \delta^2\frac{k+\mu}{\mu}\left[\delta^2\frac{\partial^2 v}{\partial x^2} + \frac{\partial^2 v}{\partial y^2}\right] - \delta^2\frac{a^2}{k_1}v \tag{13}$$

$$Re\ \delta\ \frac{\mu J}{k}\left[u\frac{\partial \Omega}{\partial x} + v\frac{\partial \Omega}{\partial y}\right] = -2\Omega + \left[\delta^2\frac{\partial v}{\partial x} - \frac{\partial u}{\partial y}\right] + \frac{\gamma_1}{a^2 k}\left[\delta^2\frac{\partial^2 \Omega}{\partial x^2} + \frac{\partial^2 \Omega}{\partial y^2}\right] \tag{14}$$

$$Re\ P_r\delta\left[u\frac{\partial \theta}{\partial x} + v\frac{\partial \theta}{\partial y}\right] = \left[\delta^2\frac{\partial^2 \theta}{\partial x^2} + \frac{\partial^2 \theta}{\partial y^2}\right] + N_b\left(\delta^2\frac{\partial \varphi}{\partial x}\frac{\partial \theta}{\partial x} + \frac{\partial \varphi}{\partial y}\frac{\partial \theta}{\partial y}\right) + N_t\left(\delta^2\left(\frac{\partial \theta}{\partial x}\right)^2 + \left(\frac{\partial \theta}{\partial y}\right)^2\right) - \gamma P_r\theta \tag{15}$$

$$\delta S_c\left[u\frac{\partial \varphi}{\partial x} + v\frac{\partial \varphi}{\partial y}\right] = \left[\delta^2\frac{\partial^2 \varphi}{\partial x^2} + \frac{\partial^2 \varphi}{\partial y^2}\right] + \frac{N_t}{N_b}\left[\delta^2\frac{\partial^2 \theta}{\partial x^2} + \frac{\partial^2 \theta}{\partial y^2}\right] - SS_c\varphi \tag{16}$$

The dimensionless boundary conditions are:

$$\left.\begin{array}{l} u = 0\,,\ \Omega = 0\ ,\ \theta = 0 \text{ and } \varphi = 0 \quad \text{at} \quad y = -h \\ u = 0\,,\ \Omega = 0\ ,\ \theta = 1 \text{ and } \quad \varphi = 1 \quad \text{at } y = h \end{array}\right\} \tag{17}$$

For long wavelength(i.e, $\delta \ll 1$) and low Reynolds number (i.e., $Re \to 0$) the system of our equations (12-16) can be reduced to:

$$\frac{1}{1-N}\frac{\partial^2 u}{\partial y^2} + \frac{N}{1-N}\frac{\partial \Omega}{\partial y} - a_1^2 u = \frac{\partial P}{\partial x} \tag{18}$$

$$\frac{\partial P}{\partial y} = 0 \tag{19}$$

$$\frac{2-N}{m^2}\frac{\partial^2 \Omega}{\partial y^2} - \frac{\partial u}{\partial y} - 2\Omega = 0 \tag{20}$$

$$\frac{\partial^2\theta}{\partial y^2} + N_b \frac{\partial \varphi}{\partial y}\frac{\partial \theta}{\partial y} + N_t \left(\frac{\partial \theta}{\partial y}\right)^2 - \gamma \mathrm{P_r}\theta = 0 \tag{21}$$

$$\frac{\partial^2\varphi}{\partial y^2} + \frac{N_t}{N_b}\frac{\partial^2\theta}{\partial y^2} - SS_c\varphi = 0 \tag{22}$$

From equation (19), it is clear that P is independent of y. Therefore equation (18) can be written as:

$$\frac{1}{1-N}\frac{\partial^2 u}{\partial y^2} + \frac{N}{1-N}\frac{\partial \Omega}{\partial y} - a_1^2 u = \frac{dP}{dx} \tag{23}$$

By using equations (2) and (3) with the help of the wall equation (1) we can write:

$$\frac{dP}{dx} = -\epsilon[(2\pi)^3 \cos 2\pi(x-t)(E_1+E_2) - (2\pi)^2 E_3 \sin 2\pi(x-t)] \tag{24}$$

Where $N = \frac{k}{k+\mu}$ is the coupling number, $a_1^2 = \frac{a^2}{k_1}$ is the porosity parameter, $m^2 = \frac{a^2 k(2\mu+k)}{\gamma_1(\mu+k)}$ is the micropolar parameter, $E_1 = -\frac{T_2 a^3}{\mu c \lambda^3}$ is the membrane tension parameter of the wall, $E_2 = \frac{M_2 c a^3}{\mu\lambda^3}$ is the mass characterizing parameter of the wall, $E_3 = \frac{C_2 a^3}{\mu\lambda^2}$ is the damping parameter of the wall, $\epsilon = \frac{b}{a}$ is the amplitude ratio , $P_r = \frac{\mu c_f}{k_T}$ is the Prandtl number, $S_c = \frac{ca}{D_B}$ is the Schmidt number, $Re = \frac{\rho_f c a}{\mu}$ is the Reynolds number, $\gamma = \frac{Q_o a^2}{\mu c_f}$ is the coefficient of heat absorption, $S = \frac{k_2 a}{c}$ is the coefficient of chemical reaction, $N_b = \frac{(\rho c)_p D_B(\varphi_1-\varphi_o)}{(\rho c)_f \alpha}$ is the Brownian parameter, $\alpha = \frac{k}{(\rho c)_f}$ and $N_t = \frac{(\rho c)_p D_T(T_1-T_o)}{(\rho c)_f \alpha T_o}$ is the thermophoresis parameter.

3. Method of solution

Introducing the stream functions ψ such that:

$$u = \frac{\partial \psi}{\partial y}$$

Then (20) and (23) takes the form:

$$\frac{\partial^3\psi}{\partial y^2} - a_1^2(1-N)\frac{\partial \psi}{\partial y} + N\frac{\partial \Omega}{\partial y} - p_1 = 0 \tag{25}$$

$$\frac{2-N}{m^2}\frac{\partial^2 \Omega}{\partial y^2} - \frac{\partial^2 \psi}{\partial y^2} - 2\Omega = 0 \tag{26}$$

Where $p_1 = (1-N)\frac{dP}{dx}$

Using the condition $\psi = 0$ at $y = 0$, the general solution of equations (25) and (26) by using the boundary conditions (17) are given by:

$$\psi(y) = e^{-\beta_5 y}c_1 + e^{\beta_5 y}c_2 + e^{-\beta_6 y}c_3 + e^{\beta_6 y}c_4 - \frac{c_5 + y\beta_4}{\beta_3} \tag{27}$$

$$u(y) = -\frac{\beta_4}{\beta_3} - e^{-y\beta_5}c_1\beta_5 + e^{y\beta_5}c_2\beta_5 - e^{-y\beta_6}c_3\beta_6 + e^{y\beta_6}c_4\beta_6 \tag{28}$$

$$\Omega(y) = \frac{e^{-\frac{\sqrt{2}y}{\sqrt{\beta_1}} - y(\beta_5+\beta_6)}\left(e^{y\left(\frac{\sqrt{2}}{\sqrt{\beta_1}}+\beta_6\right)}c_1\beta_5^2\beta_3 + e^{y\left(\frac{\sqrt{2}}{\sqrt{\beta_1}}+2\beta_5+\beta_6\right)}c_2\beta_5^2\beta_3 + e^{y\beta_5}\beta_7\left(e^{\frac{\sqrt{2}y}{\sqrt{\beta_1}}}(c_3 + e^{2y\beta_6}c_4)\beta_6^2 + e^{y\beta_6}\left(c_5 + e^{\frac{2\sqrt{2}y}{\sqrt{\beta_1}}}c_6\right)\beta_8\right)\right)}{\beta_7\beta_8} \tag{29}$$

The homotopy perturbation method is a series expansion method used to solve nonlinear ordinary and partial differential equations. On the basis of the homotopy perturbation method [27] we can write equations (21) and (22) as follows:

$$H(q,\theta) = (1-q)[L(\theta) - L(\theta_{10})] + q\left[L(\theta) + N_b\frac{\partial\varphi}{\partial y}\frac{\partial\theta}{\partial y} + N_t\left(\frac{\partial\theta}{\partial y}\right)^2 - \gamma \mathrm{P_r}\theta\right] \tag{30}$$

$$H(q,\varphi) = (1-q)[L(\varphi) - L(\varphi_{10})] + q\left[L(\varphi) + \frac{N_t}{N_b}\frac{\partial^2\theta}{\partial y^2} - SS_c\varphi\right] \tag{31}$$

With $L = \frac{\partial^2}{\partial y^2}$ is a linear operator, the initial approximation θ_{10} and φ_{10} can be defined as:

$$\theta_{10}(x,y) = \frac{y+h}{2h} = \varphi_{10}(x,y) \tag{32}$$

The basic assumption is that the solution of equations (30) and (31) can be expanded as a power series in q

$$\theta(y,q) = \theta_o + q\theta_1 + q^2\theta_2 + \cdots \quad (33)$$

$$\varphi(y,q) = \varphi_o + q\varphi_1 + q^2\varphi_2 + \cdots \quad (34)$$

The solution of temperature and nanoparticle phenomenon (for $q = 1$) are constructed as follows:

$$\theta(x,y) = \frac{1}{480h^3}(240h^3c_7(2 + y^2\gamma P_r) + 40h^2yc_8(12h + y(-3N_b - 6N_t + 2hy\gamma P_r)) + 2(120h^2(h + y) + 240h^3c_{11} + y(240h^3c_{12} + 5y(yN_b^2 + N_t(-6h + yN_t) + 2N_b(-3h(1 + 2hc_{10}) + yN_t)) - 5hy\gamma(-4h(3h + y) + y(2h + y)(N_b + N_t))P_r + h^2y^3(5h + y)\gamma^2P_r^2)) - 5hSy^3(4h + y)N_bS_c) \quad (35)$$

$$\varphi(x,y) = \frac{1}{480h^3N_b}(-10y^3N_b^2N_t + 2N_b(5(24h^2(h + y + 2h(c_9 + c_{13} + y(c_{10} + c_{14}))) + 6hy^2(1 + 2h(c_8 + c_{10}))N_t - 2y^3N_t^2 + hy^3(2h + y)\gamma N_tP_r) + 5hSy^2(4h(3h + y + 6hc_9 + 2hyc_{10}) + y(2h + y)N_t)S_c + h^2S^2y^4(5h + y)S_c^2) + y^2N_t(-10yN_t^2 + 5hN_t(12 + 48hc_8 + y(2(2h + y)\gamma P_r + SyS_c)) - 2h^2\gamma P_r(20(3h + y) + 120hc_7 + y(40hc_8 + y(5h + y)(\gamma P_r + SS_c))))) \quad (36)$$

Where $c_1 \rightarrow c_{14}$ and $\beta_1 \rightarrow \beta_8$ are defined in the appendix.

4. Results and discussion

In order to get a clear insight of the effects of heat absorption, chemical reaction and wall properties on peristaltic flow of micropolar fluid with nanoparticles through porous medium in a symmetric horizontal channel, we have computed numerical values of velocity, microrotation velocity, temperature and nanoparticle phenomenon for different values of various parameters entering the problem.

4.1 Velocity and microrotation velocity distributions. The velocity u and the microrotation velocity Ω of the flow field are found to change more or less with the variation of the flow parameters. The effect of the flow parameters on these distributions are analyzed with the help of figures (2)-(12).

Fig. (2) display the effect of the porous parameter a_1 on the velocity distribution. The magnitude of the velocity decreases with the increase in a_1. It is also observed that the

maximum velocity occurs at the center of the channel. This result in agreement with the physical expectation, since the porous represents an obstacle to flow and therefore, reduced its velocity.

Figs. (3) and (4) depict the effects of the coupling number N on the velocity and the microrotation velocity distributions. It is found that the velocity decrease with the increase of the coupling number N. While the microrotation velocity increase with the increase of the coupling number N near the lower wall and the inverse effect occur near the upper wall.

Figs. (5) and (6) illustrate the velocity and the microrotation velocity distributions for several values of the micropolar parameter m. It's seen that the increase of the micropolar parameter m increase the velocity of the flow field. It also noted that the difference of the velocity for different values of m becomes greater with increasing the normal axis y and reaches the maximum value at the center of the channel. From fig. (6) it is observed that an increase in m decrease the microrotation velocity near the lower wall of the channel whereas it increases Ω near the upper wall of the channel.

Figs. (7)-(9) display the effects of wall parameters on the velocity distribution. The rigid nature of the wall is represented by the parameter E_1, which depends on the wall tension and E_2 represents the stiffness property of the wall. E_3 represents the dissipative feature of the wall. The choice $E_3 = 0$ implies that the wall moves up and down with no damping force on it, and therefore, indicates the case of elastic walls. The effects of the rigid nature and the stiffness property of the walls on the velocity distribution for the elastic walls ($E_3 = 0$) is shown in figures (7) and (8). It can be seen from these figures that the velocity increase by increasing the tension parameter E_1 and the mass characterizing parameter E_2. The effect of the dissipative walls on the velocity is given in figure (9). This figure show that, as the dissipative nature of the walls E_3 increase, the velocity decreased.

Figs. (10) - (12) illustrate the effects of wall parameter on the microrotation velocity distribution. It is seen that microrotation velocity Ω at fixed values of y decreases as E_1 and E_2 increase, this occurs near the lower wall and the inverse effect occurs near the upper wall which indicated graphically through figures (10) and (11). Figure (12) shows

the variation of the microrotation velocity Ω for different values of the damping parameter E_3. It is clear that Ω increase by increasing the values of the damping parameter E_3 near the lower wall and the inverse effect occurs near the upper wall.

4.2 Temperature distribution. The temperature of the flow field is mainly affected by four flow parameters, namely, Prandtl number P_r, heat absorption coefficient γ, the Brownian parameter N_b and the thermophoresis parameter N_t. The effects of these parameters on the temperature of the flow field are shown in figures (13)-(16) respectively.

Figs. (13) and (14) depict the effects of the Prandtl number P_r and the coefficient of heat absorption γ on the temperature distribution. The Prandtl number is the ratio of momentum diffusion to heat diffusion. It is a measure of the relative importance of viscosity and heat conducting in a flow field. Thus, as the Prandtl number increases, the viscous forces dominate over heat conducting and hence, the temperature decreases. The variation in the temperature distribution for different values of coefficient of heat absorption γ is given in figure (14). It is noticed that an increase in the values of γ leads to decrease in the temperature.

Figs. (15) and (16) display the effects of the Brownian parameter N_b and the thermophoresis parameter N_t on the temperature distribution. There is a substantial increase in the temperature with an increase in N_b and N_t. As the Brownian motion and thermophoretic effects strengthen, this corresponds to the effective movement of nanoparticles from the wall to the fluid which results in the significant increase in the temperature.

4.3 Nanopaticles phenomena distribution. The nanoparticles phenomena distribution of the flow field is affected by four parameters, namely, the Schmidt number S_c, the chemical reaction coefficient S, the Brownian parameter N_b and the thermophoresis parameter N_t

Fig. (17) illustrates the nanoparticles phenomena distribution against y for several values of the Schmidt number S_c. The Schmidt number quantifies the relative

effectiveness of momentum and mass transport by diffusion in hydrodynamic and nanoparticles. As the Schmidt number increase the nanoparticles phenomena decrease.

Figs. (18) Shows the effect of the coefficient of chemical reaction S on the nanoparticles phenomena. It is clear that nanoparticles phenomena decrease as the coefficient of chemical reaction S increase.

Figs. (19) and (20) display the effects of the Brownian parameter N_b and the thermophoresis parameter N_t on the nanoparticles phenomena. There is a substantial increase in the nanoparticles phenomena with an increase in N_b. While the nanoparticles phenomena decrease by increasing the thermophoresis parameter N_t.

5. Conclusion

Wall properties on the peristaltic transport of micropolar fluid with nanoparticles through porous medium in a symmetric channel under the effects of heat absorption and chemical reaction are addressed. Under the assumption of long wavelength and low Reynolds number, the expressions of velocity and microrotation velocity are obtained in closed form, while the solutions of temperature and nanoparticles equations are obtained by using homotopy perturbation method. It believed that the present work will serve for understanding more complex problems including the various physical effects investigated in the present problem. The main results are summarized as follows:

(1) The velocity of the flow field decrease in both region of the channel by increasing the porous parameter a_1.

(2) microrotation Ω velocity increase with the increase of the coupling number N near the lower wall and the inverse effect occur near the upper wall.

(3) The effects of the rigid nature and the stiffness property of the walls on the velocity distribution for the elastic walls ($E_3 = 0$) increase the velocity.

(4) The increase of Prandtl number leads to the temperature decreases.

(5) The temperature increase with an increase in N_b and N_t.

(6) Increasing the magnitude of chemical reaction coefficient S led to decrease in the nanoparicles phenomena.

(7) The nanoparticles phenomena increase with an increase in N_b. While the nanoparticles phenomena decrease by increasing the thermophoresis parameter N_t.

6. Caption of figures

Figure (2). The velocity distribution u is plotted against y for different values of a_1 when $m = 6$, $N = 0.2$, $\epsilon = 0.5,\ x = \pi,\ t = \pi$, $E_1 = .01,\ E_2 = .01, E_3 = 0$.

Figure (3). The velocity distribution u is plotted against y for different values of N when $m = 6$, a_1 =0.2, $\epsilon = 0.5, x = \pi, t = \pi, E_1 = .01$, $E_2 = .01, E_3 = 0$.

Figure (4). The microrotation velocity distribution Ω is plotted against y for different values of N when $m = 6$, a_1 =0.2, $\epsilon = 0.5, x = \pi, t = \pi, E_1 = .01$, $E_2 = .01, E_3 = 0$.

Figure (5). The velocity distribution u is plotted against y for different values of m when $N = 0.2$, a_1 =0.2, $\epsilon = 0.5, x = \pi, t = \pi, E_1 = .01$, $E_2 = .01, E_3 = 0$.

Figure (6). The microrotation velocity distribution Ω is plotted against y for different values of m when $N = 0.2$, a_1 =0.2, $\epsilon = 0.5, x = \pi, t = \pi, E_1 = .01$, $E_2 = .01, E_3 = 0$

Figure (7). The velocity distribution u is plotted against y for different values of E_1 when $N = 0.2$, a_1 =0.2, $m = 6$, $\epsilon = 0.5, x = \pi, t = \pi, E_2 = .01, E_3 = 0$.

Figure (8). The velocity distribution u is plotted against y for different values of E_2 when $N = 0.2$, a_1 =0.2, $m = 6$, $\epsilon = 0.5, x = \pi, t = \pi, E_1 = .01, E_3 = 0$.

Figure (9). The velocity distribution u is plotted against y for different values of E_3 when $N = 0.2$, a_1 =0.2, $m = 6$, $\epsilon = 0.5, x = .11, t = .1, E_1 = .01, E_2 = .01$.

Figure (10). The microrotation velocity distribution Ω is plotted against y for different values of E_1 when $N = 0.2$, a_1 =0.2, $m = 6$, $\epsilon = 0.5, x = \pi, t = \pi, E_2 = .01, E_3 = 0$.

Figure (11). The microrotation velocity distribution Ω is plotted against y for different values of E_2 when $N = 0.2$, a_1 =0.2, $m = 6$, $\epsilon = 0.5, x = \pi, t = \pi, E_1 = .01, E_3 = 0$.

Figure (12). The microrotation velocity distribution Ω is plotted against y for different values of E_3 when $N = 0.2$, a_1 =0.2, $m = 6$, $\epsilon = 0.5,\ x = .11, t = .1,\ E_1 = .01, E_2 = .01$.

Figure (13). The temperature θ is plotted against y for different values of P_r when $S_c = 0.15, S = 2, x = \pi,\ t = \pi,\ \epsilon = .5, N_b = 1.5$, $N_t = 1$, $\gamma = .5$.

Figure (14). The temperature θ is plotted against y for different values of γ when $\mathrm{Pr} = .71$, $S_c = 0.15, S = 2, x = \pi,\ t = \pi,\ \epsilon = .5, N_b = 1.5$, $N_t = 1$.

Figure (15). The temperature θ is plotted against y for different values of N_b when $S_c = 0.15, S = 2, x = \pi,\ t = \pi,\ \epsilon = .5, \mathrm{Pr} = .71$, $N_t = 1$, $\gamma = .5$.

Figure (16). The temperature θ is plotted against y for different values of N_t when $S_c = 0.15, S = 2, x = \pi,\ t = \pi,\ \epsilon = .5, N_b = 1.5$, $\mathrm{Pr} = .71$, $\gamma = .5$.

Figure (17).The concentration φ is plotted against y for different values of S_C when $P_r = .7$, $\gamma = .5,\ S = 2,\ x = \pi,\ t = \pi,\ \epsilon = .5,\ N_b = 1.5,\ N_t = 1$.

Figure (18).The concentration φ is plotted against y for different values of S when $P_r = .7$, $\gamma = .5,\ S_c = 0.15,\ x = \pi,\ t = \pi,\ \epsilon = .5,\ N_b = 1.5,\ N_t = 1$.

Figure (19).The concentration φ is plotted against y for different values of N_b when $P_r = .7$, $\gamma = .5,\ S_c = 0.15,\ x = \pi,\ t = \pi,\ \epsilon = .5,\ S = 2,\ N_t = 1$.

Figure (20).The concentration φ is plotted against y for different values of N_t when $P_r = .7$, $\gamma = .5,\ S_c = 0.15,\ x = \pi,\ t = \pi,\ \epsilon = .5,\ S = 2,\ N_b = 1.5$.

References

[1] A. De Risi and M. Milanese," High efficiency nanofluid cooling system for wind turbines", Thermal Science, 18, (2014), 543-554.

[2] K. Prasad, N. Subadra, M. Srinivas, "Peristaltic transport of a nanofluid in an inclined tube", American Journal of Computational and Applied Mathematics, 5, (2015), 117-128.

[3] K. Nowar," Peristaltic flow of a nanofluid under the effect of hall current and porous medium", Mathematical Problems in Engineering,(2014), 1-15.

[4] S. Akram, S. Nadeem, A. Ghafoor, C. Lee," Consequences of nanofluid on peristaltic flow in an asymmetric channel", IJBAS, 12,(2012), 75-96.

[5] I. Mahbubul, R. Saidur, M. Amalina," Latest developments on the viscosity of nanofluids", International Journal of Heat and Mass Transfer, 55, (2012), 874-885.

[6] M. Mustafa, S. Hina, T. Hayat, A. Alsaedi," Influence of wall properties on the peristaltic flow of a nanofluid: analytical and numerical solutions", International Journal of Heat and Mass Transfer, 55,(2012), 4871-4877.

[7] N. Akbar, S. Nadeem, Z. Khan," Numerical simulation of peristaltic flow of a Carreau nanofluid in an asymmetric channel", Alexandria Engineering Journal, (2013), 1-7.

[8] M. Krishnamurthy, B. Prasannakumara, B. Gireesha," Effect of chemical reaction on MHD boundary layer flow and melting heat transfer of Williamson nanofluid in porous medium", Engineering Science and Technology, 19, (2016), 53-61.

[9] A. Eringen," Theory of micropolar fluids", Journal of Mathematics and Mechanics, 16, (1966), 1-16.

[10] S. Nadeem, Abdul Rehman, K. Vajravelu," Axisymmetric stagnation flow of a micropolar nanofluid in a moving cylinder", Mathematical Problems in Engineering, (2012), 1-18.

[11] O. Beg, R. Bhargava, S. Rawat, E. Kahya, "Numerical study of micropolar convective heat and mass transfer in a non-Darcy porous regime with Soret and Dufour diffusion effects", Emirates Journal for Engineering Research, 2, (2008), 51-66.

[12] A. Ishak, R. Nazar, I. Pop , "Flow of a micropolar fluid on a continuous moving surface", Arch. Mech., 6, 2006, 529–541.

[13] A. Bakier," Natural convection heat and mass transfer in a micropolar fluid-saturated non-Darcy porous regime with radiation and thermophoresis effects", Bakier, A. Y.: Natural Convection Heat and Mass Transfer in a Micropolar, 2, (2011), 317-326.

[14] D. Tripathi, M. Chaube, P. Gupta, "Stokes flow of micropolar fluids by peristaltic pumping though tube with slip boundary condition", Appl. Math. Mech. -Engl. Ed., 12, (2011), 1587–1598.

[15] P. Biswas, A. Jony, A. Islam, "MHD micropolar fluid flow through vertical plate with heat generation", Academic Research International, 1, (2012), 60-74.

[16] A. Abd-Allaa , G. Yahyab, H. Al -Osaimia ," Peristaltic transport of micropolar fluid in a tubes under influence of magnetic field and rotation", International Journal of Engineering and Technology,1 , (2011), 22-39.

[17] H. El-Arabawy, "Effect of suction/injection on flow of micropolar fluid past a continuously moving plate in the presence of radiation", International Journal of Heat and Mass Transfer, 46, (2003), 1471–1477.

[18] M. Abou-zeid, "Effects of thermal-diffusion and viscous dissipation on peristaltic flow of micropolar non-Newtonian nanofluid: application of homotopy perturbation method", Results in Physics, 6, (2016), 481-498.

[19] N. Eldabe, M. Abou-zeid, " The wall properties effect on peristaltic transport of micropolar non-Newtonian fluid with heat and mass transfer", Mathematical Problems in Engineering, (2010), 1-27.

[20] C. Sankad, G. Radhakrishnamacharya, "Influence of wall properties on the peristaltic motion of a Herschel-Bulkley fluid in channel", ARPN J. of Engineering and Applied Sciences, 10, (2009), 27-35.

[21] S. Sreenadh, S. Rajender, Y. Kumar," Flow of Herschel-Bulkley fluid in an inclined flexible channel lined with porous material under peristalsis", International J. of Innovative Technology and Creative Engineering, 7,(2011), 24-35.

[22] C. Vasudev, U. Rajeswara, M. Subba, G. Prabhakara, "Effect of heat transfer on peristaltic transport of a Newtonian fluid through a porous medium in an asymmetric vertical channel ", European J. of Scientific Research, 1, (2010), 79-92.

[23] C. Vasudev, U. Rajeswara, G. Prabhakara, M. Subba, "Peristaltic flow of a Newtonian fluid through a porous medium in a vertical tube under the effect of magnetic field ", Int. J. Cur. Sci. Res., 3, (2011), 105-110.

[24] A. Abd El Naby, M. El-Kareem, " The flow separation through peristaltic motion for Power-law fluid in uniform tube", Applied Mathematical Sciences,26, (2007),1249-1263.

[25] T. Hayat, M. Javed," Exact solutions to peristaltic transport of Power-law fluid in asymmetric channel with compliant walls", Appl. Math. Mech. Eng. Ed., 10, (2010), 1231-1240.

[26] A. Kavitha, R. Hemadri, S. Sreenadh, R. Saravana, " Peristaltic flow of Williamson fluid in an asymmetric channel through porous medium", International J. of Innovative Technology and Creative Engineering, 1, (2011), 48-53.

[27] T. Hayat, F. Abbasi, A. Hendi, " Heat transfer analysis for peristaltic mechanism in variable viscosity fluid ", Chin. Phys. Lett., 4, (2011), 1-3.

Appendix

$$\beta_1=\frac{2-\alpha}{m^2},\beta_2=a_1^2(1-\alpha)+m^2,\beta_3=2a_1^2(1-\alpha),\beta_4=2p_1,\beta_5=\frac{\sqrt{\beta_2-\sqrt{\frac{\beta_1\beta_2^2-4\beta_3}{\beta_1}}}}{\sqrt{2}},\beta_6=\sqrt{\frac{\beta_2}{2}+\frac{1}{2}\sqrt{\beta_2^2-\frac{4\beta_3}{\beta_1}}},\beta_7=\left(-2+\beta_1\beta_5^2\right),\beta_8=(-2+\beta_1\beta_6^2)$$

$$c_1=\frac{e^{h\beta_5}(-1+e^{2h\beta_6})\beta_4\beta_6}{\beta_3\beta_5(-\beta_5+e^{2h\beta_5}\beta_5-e^{2h\beta_6}\beta_5+e^{2h\beta_5+2h\beta_6}\beta_5+\beta_6+e^{2h\beta_5}\beta_6-e^{2h\beta_6}\beta_6-e^{2h\beta_5+2h\beta_6}\beta_6)}$$

$$c_2=-\frac{e^{h\beta_5}(-1+e^{2h\beta_6})\beta_4\beta_6}{\beta_3\beta_5(-\beta_5+e^{2h\beta_5}\beta_5-e^{2h\beta_6}\beta_5+e^{2h\beta_5+2h\beta_6}\beta_5+\beta_6+e^{2h\beta_5}\beta_6-e^{2h\beta_6}\beta_6-e^{2h\beta_5+2h\beta_6}\beta_6)}$$

$$c_3=\frac{e^{h\beta_6}(-1+e^{2h\beta_5})\beta_4\beta_5}{\beta_3\beta_6(\beta_5-e^{2h\beta_5}\beta_5+e^{2h\beta_6}\beta_5-e^{2h\beta_5+2h\beta_6}\beta_5-\beta_6-e^{2h\beta_5}\beta_6+e^{2h\beta_6}\beta_6+e^{2h\beta_5+2h\beta_6}\beta_6)}$$

$$c_4=-\frac{e^{h\beta_6}(-1+e^{2h\beta_5})\beta_4\beta_5}{\beta_3\beta_6(\beta_5-e^{2h\beta_5}\beta_5+e^{2h\beta_6}\beta_5-e^{2h\beta_5+2h\beta_6}\beta_5-\beta_6-e^{2h\beta_5}\beta_6+e^{2h\beta_6}\beta_6+e^{2h\beta_5+2h\beta_6}\beta_6)}$$

$$c_5=(\mathrm{Csch}[\frac{2\sqrt{2}h}{\sqrt{\beta_1}}](-(\mathrm{Sinh}[h(\frac{\sqrt{2}}{\sqrt{\beta_1}}+\beta_6)]c_3+\mathrm{Sinh}[\frac{\sqrt{2}h}{\sqrt{\beta_1}}-h\beta_6]c_4)(-2+\beta_1\beta_5^2)\beta_6^2+\mathrm{Sinh}[h(\frac{\sqrt{2}}{\sqrt{\beta_1}}+\beta_5)]c_1\beta_5^2(2-\beta_1\beta_6^2)+\mathrm{Sinh}[\frac{\sqrt{2}h}{\sqrt{\beta_1}}-h\beta_5]c_2\beta_5^2(2-\beta_1\beta_6^2)))/((-2+\beta_1\beta_5^2)(-2+\beta_1\beta_6^2))$$

$$c_6 = (\text{Csch}[\frac{2\sqrt{2}h}{\sqrt{\beta_1}}](-(\text{Sinh}[\frac{\sqrt{2}h}{\sqrt{\beta_1}} - h\beta_6]c_3 + \text{Sinh}[h(\frac{\sqrt{2}}{\sqrt{\beta_1}} + \beta_6)]c_4)(-2 + \beta_1\beta_5^2)\beta_6^2 + \text{Sinh}[\frac{\sqrt{2}h}{\sqrt{\beta_1}} - h\beta_5]c_1\beta_5^2(2 - \beta_1\beta_6^2) + \text{Sinh}[h(\frac{\sqrt{2}}{\sqrt{\beta_1}} + \beta_5)]c_2\beta_5^2(2 - \beta_1\beta_6^2)))/((-2 + \beta_1\beta_5^2)(-2 + \beta_1\beta_6^2))$$

$$c_7 = \frac{1}{8}(N_b + N_t - 2h^2\gamma P_r), \quad c_8 = -\frac{1}{12}h\gamma P_r$$

$$c_9 = -\frac{N_bN_t+N_t^2-2h^2\gamma N_tP_r+2h^2SN_bS_c}{8N_b}, \quad c_{10} = -\frac{-h\gamma N_tP_r+hSN_bS_c}{12N_b}$$

$$c_{11} = \frac{1}{96}(24hc_8N_b + 24hc_{10}N_b + 48hc_8N_t - 48h^2\gamma c_7P_r + 2h^2\gamma N_bP_r + 2h^2\gamma N_tP_r - 2h^4\gamma^2P_r^2 + h^2SN_bS_c)$$

$$c_{12} = -\frac{5N_b^2+10N_bN_t+5N_t^2+40h^3\gamma c_8P_r-10h^2\gamma N_bP_r-10h^2\gamma N_tP_r+h^4\gamma^2P_r^2-10h^2SN_bS_c}{240h}$$

$$c_{13} = -\frac{24hc_8N_bN_t+24hc_{10}N_bN_t+48hc_8N_t^2-48h^2\gamma c_7N_tP_r+2h^2\gamma N_bN_tP_r+2h^2\gamma N_t^2P_r-2h^4\gamma^2N_tP_r^2+48h^2Sc_9N_bS_c+2h^2SN_bN_tS_c+h^2SN_t^2S_c-2h^4S\gamma N_tP_rS_c+2h^4S^2N_bS_c^2}{96N_b}$$

$$c_{14} = -\frac{-5N_b^2N_t-10N_bN_t^2-5N_t^3-40h^3\gamma c_8N_tP_r+10h^2\gamma N_bN_tP_r+10h^2\gamma N_t^2P_r-h^4\gamma^2N_tP_r^2+40h^3Sc_{10}N_bS_c+10h^2SN_bN_tS_c-h^4S\gamma N_tP_rS_c+h^4S^2N_bS_c^2}{240hN_b}$$

Figure 2

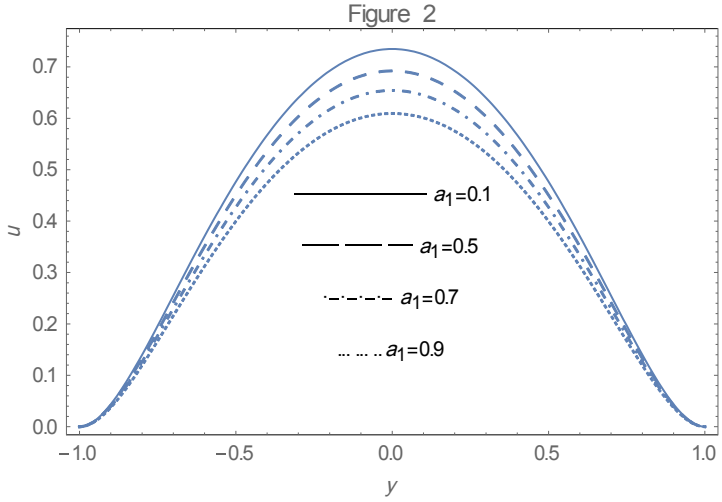

Figure 3

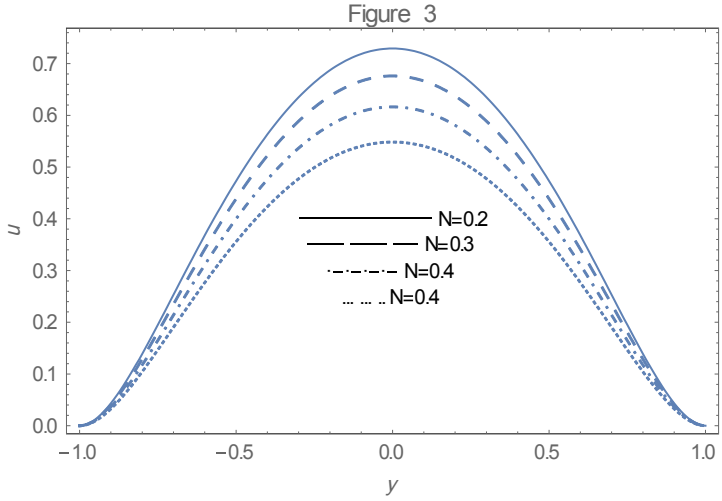

Figure 4

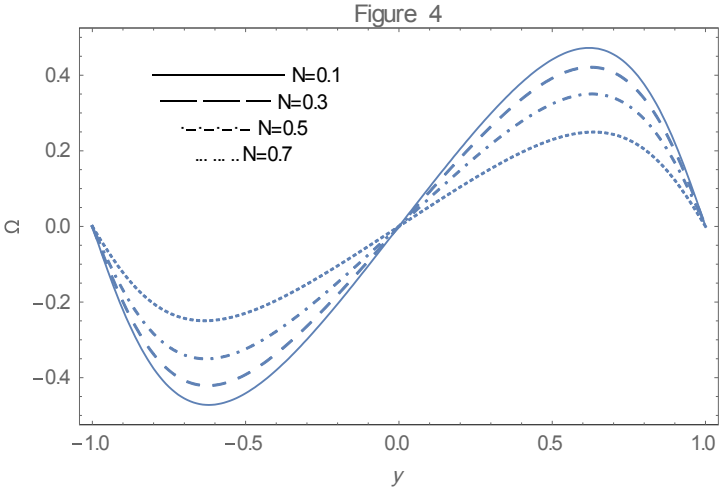

Figure 5

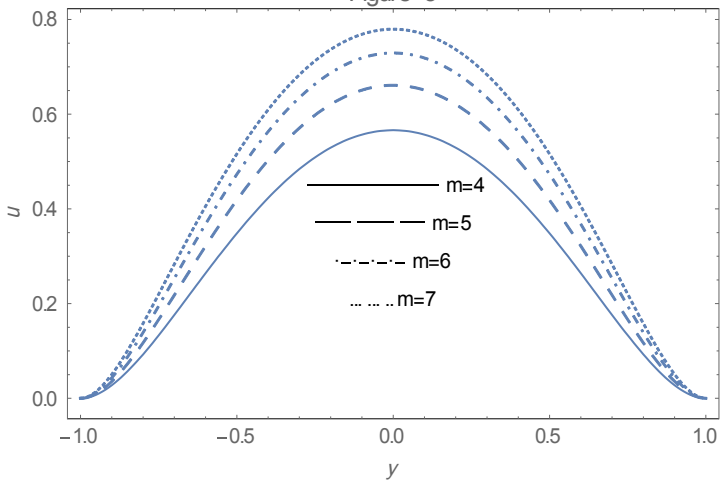

Figure 6

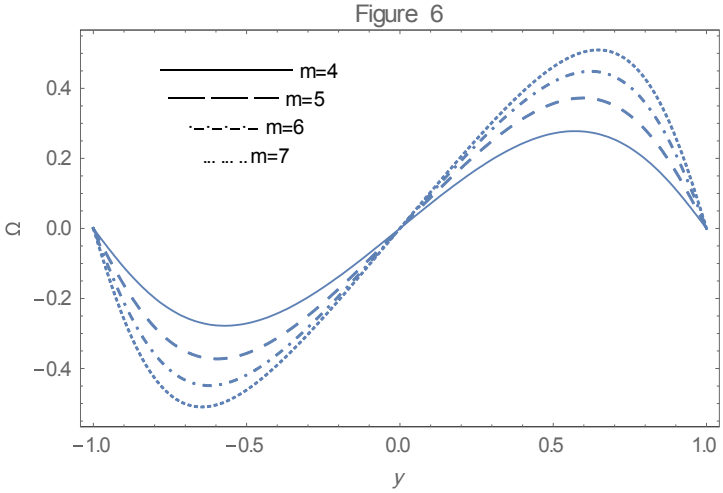

Figure 7

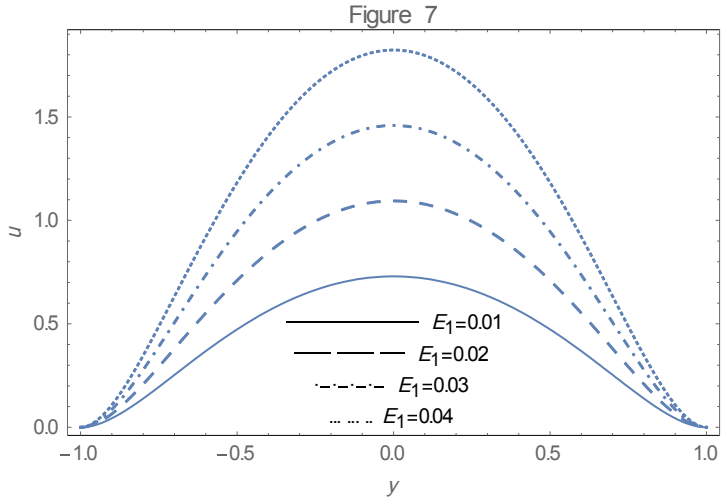

Figure 8

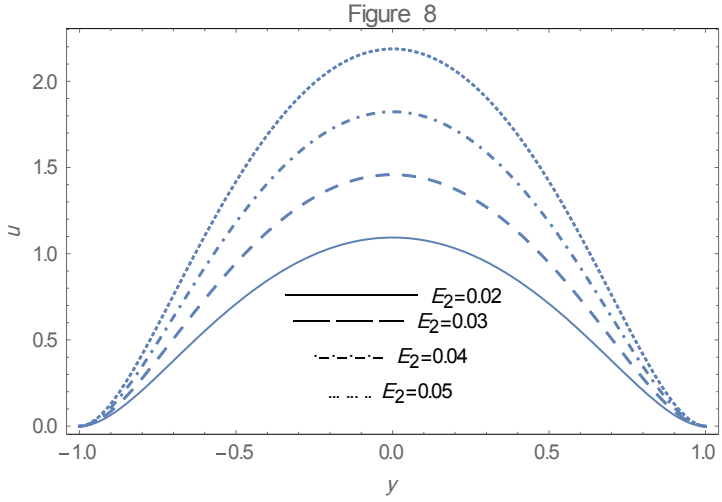

Figure 9

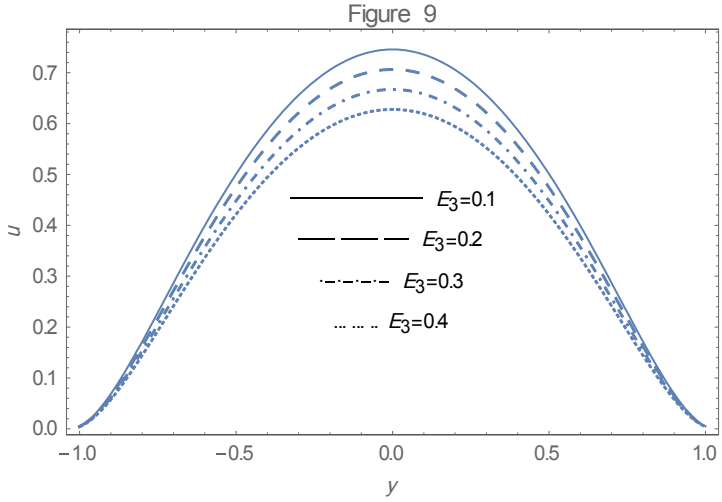

Figure 10

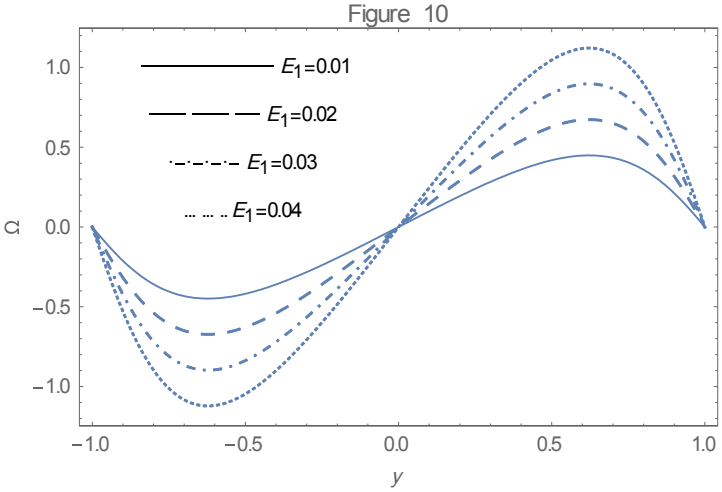

Figure 11

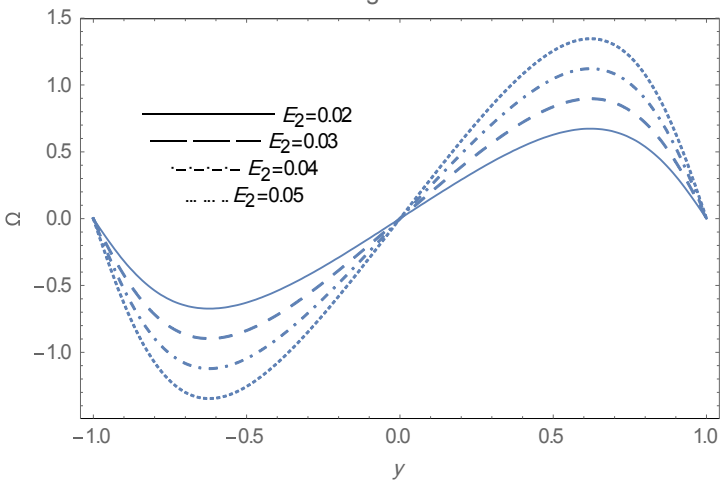

Figure 12

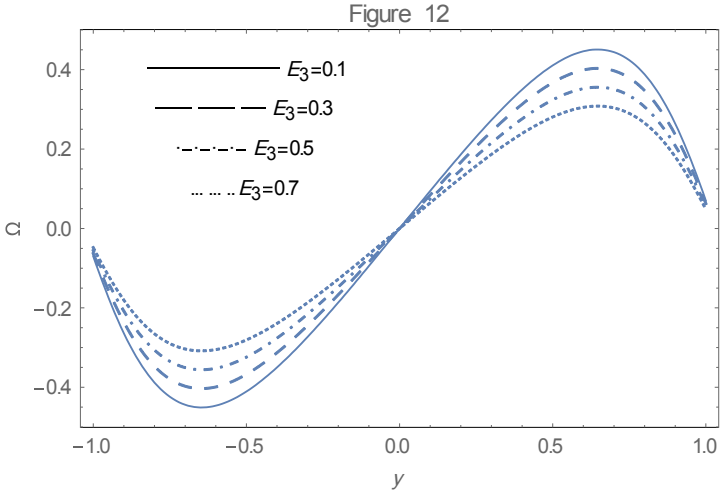

Figure 13

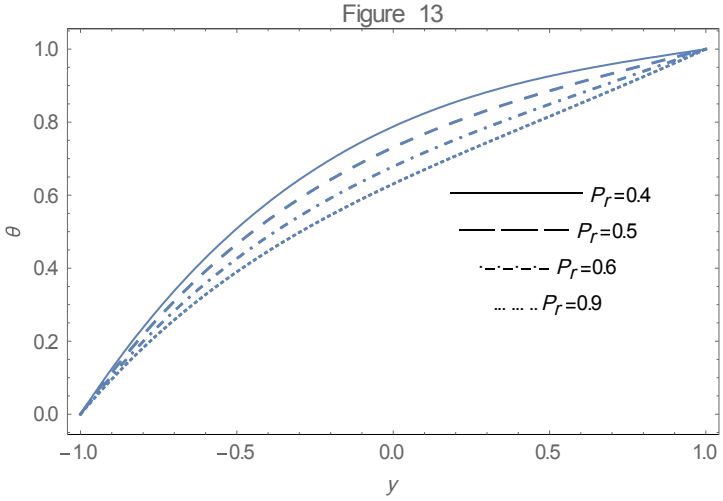

Figure 14

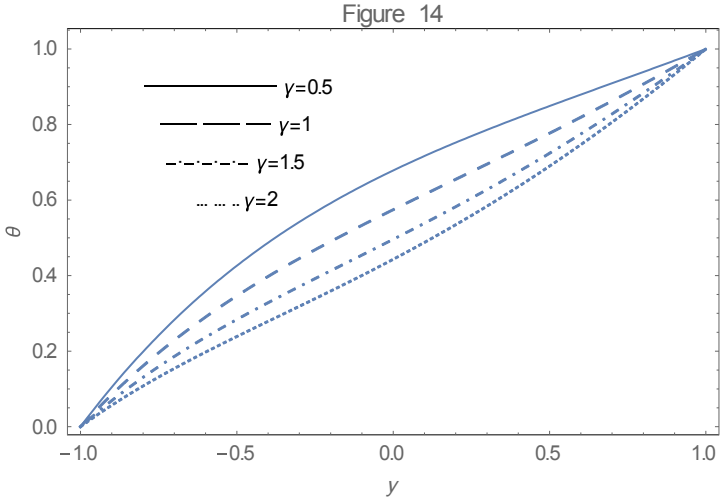

Figure 15

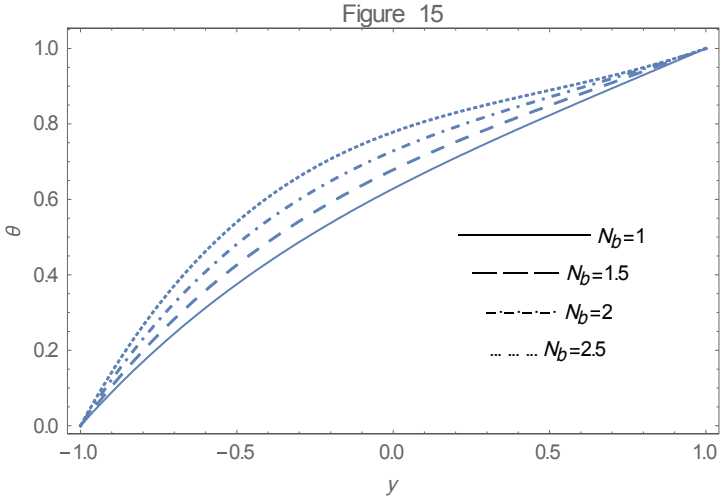

Figure 16

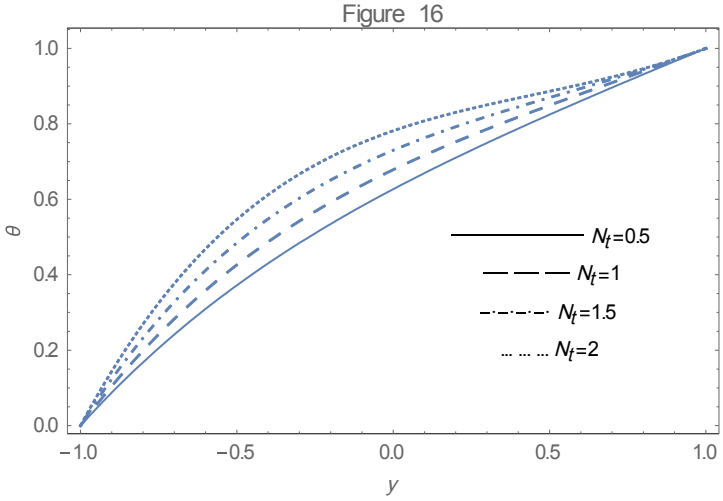

Figure 17

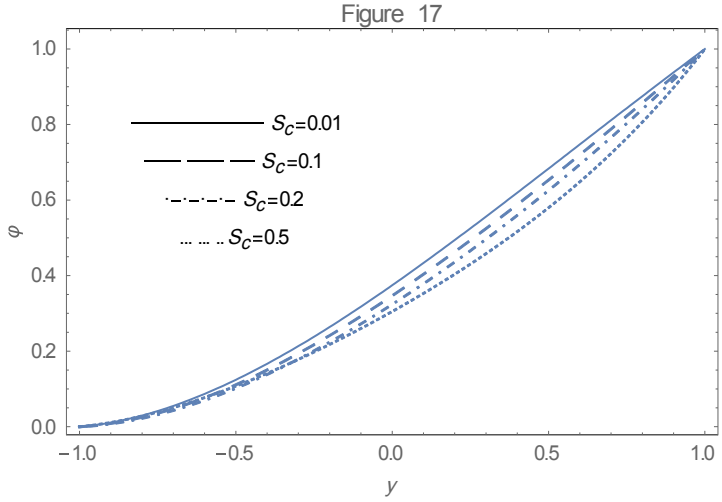

Figure 18

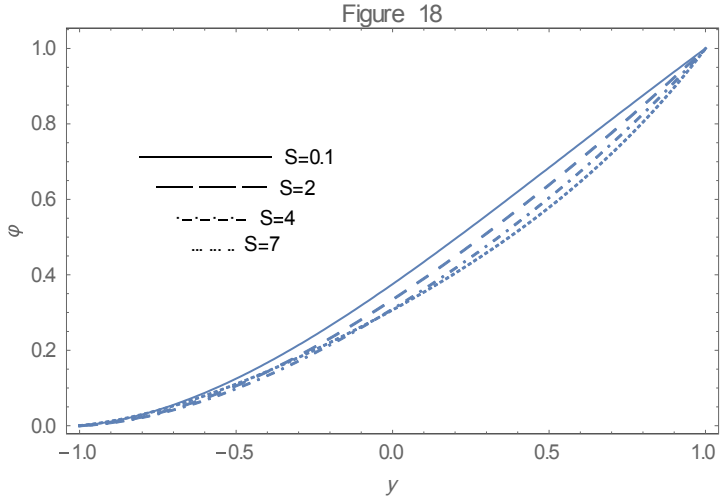

Figure 19

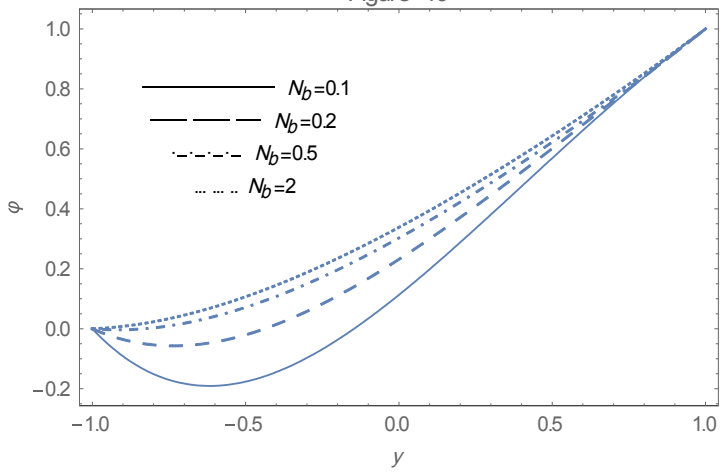

Figure 20